Synthesis of cobalt ferrite ($CoFe_2O_4$) by combustion with different concentrations of glycine

IOP Conf. Series: Materials Science and Engineering **659** (2019) 012079 doi:10.1088/1757-899X/659/1/012079

Synthesis of cobalt ferrite ($CoFe_2O_4$) by combustion with different concentrations of glycine

C G Kaufmann Junior[1, 2], R Y S Zampiva[1], A K Alves[1], C P Bergmann[1, 2] and L Giorgini[3]

[1] Post-Graduation Program in Mining, Metallurgy and Materials Engineering (PPGE3M), Federal University of Rio Grande do Sul, Osvaldo Aranha 99, 90035-190, Porto Alegre, Brazil
[2] Post-Graduation Program in Production and Transport Engineering, (PPGEP), Federal University of Rio Grande do Sul, Osvaldo Aranha 99, 90035-190, Porto Alegre, Brazil
[3] Department of Industrial Chemistry "Toso Montanari", University of Bologna, Viale del Risorgimento 4, 40136, Bologna, Italy

E-mail: gabriel.kaufmann@ufrgs.br

Abstract. Among the wide range of applications of Cobalt Ferrite ($CoFe_2O_4$), its usage for the manufacturing of modern electronic devices such as solar panels, capacitors and batteries has been studied´ lately. Hence, solar-powered vehicles, which strongly rely their performance on energy efficient electronics, is a sector that could particularly benefit from enhanced applications of such material. In this work, the synthesis of Cobalt Ferrite was studied by means of Solution Combustion Synthesis (SCS) using iron nitrate nonahydrate and cobalt nitrate hexahydrate as precursors, and glycine as fuel. The nitrates were dissolved in distilled water and placed under stirring and heating for 5 minutes; when the temperature reached 60°C, glycine was added; after complete homogenization, the solution was placed in an electric oven (400°C) until complete combustion (approximately 15 minutes). Three syntheses were carried out using different concentrations of fuel: lean, stoichiometric and rich. The product crystallite size and composition were investigated in order to determine the influence of the fuel concentration on the structure of the produced cobalt ferrite.

1. Introduction

Ferrite is a ceramic material produced from burning large proportions of iron (III) oxide (Fe_2O_3) blended with small concentrations of one or more metallic elements, such as cobalt, manganese, nickel, magnesium, and zinc [1]. Ferrites usually present a spinel structure with the formula AB_2O_4, where A and B represent various metal cations, including iron (Fe) [2].

Many studies on ferrites nanoparticles including $CoFe_2O_4$ spinel have been recently presented due to their distinct magnetic and electronic properties, which open up numerous possibilities including cancer treatment [3], biosensors [4], sensors [5], memory shape alloys [6] and water purification [7]. In addition, ferrite cobalt has been emerging as a promising material for the development of modern electronic devices, such as capacitors, sensors or high capacity batteries [8–10]. Thus this material can be particularly useful in applications related to the sustainable mobility in general and to the solar vehicles in particular. Optimizing the synthesis and usage of such material, for instance, has become a topic of interest for the design of solar-powered electric vehicles, given that power management and energy efficiency are the key aspects of such mobility branch [11-13].

Solution combustion synthesis (SCS) has been increasingly applied in the production of oxide catalysts due to the possibility of producing low-cost, highly pure and homogeneous nanostructured powders. SCS mainly consists of combining the reactants in an aqueous medium using a complexing agent (usually glycine and urea), as well as oxidizing agents (usually metal nitrates), to oxidize the fuel [14,15]. The mixture is heated to 150°C and 500°C to carry out self-ignition in a rapid combustion reaction that can reach more than 1700°C [16]. A solid product that is typically well dispersed and crystalline is formed at the end of the process [16].

The concentration ratio between the complexing agent and oxidizing agent is directly related to the final properties of the powder produced [15]. Thus, this study aims to formulate a methodology to use SCS to produce, at a low cost, homogeneous $CoFe_2O_4$ catalyst nanoparticles. For this purpose, we studied the influence of different concentrations of fuel on the product composition and morphology. With this scope, we used an experimental approach that, coupling diffractometry and microscopy, permitted relevant and unexpected results in similar situations [17-19].

2. Materials and methods

2.1 *Synthesis of cobalt ferrite*

$CoFe_2O_4$ nanostructured particles were produced by SCS with various concentrations of fuel. $Co(NO_3)_2.6H_2O$ and $Fe(NO_3)_3.9H_2O$ were employed as precursors and oxidizers, while glycine ($C_2H_5NO_2$) is used as fuel. All of the reactants were obtained from Merck. The fuel stoichiometric, rich and lean ratios were established by the chemistry of propellants method [20] and applied according to Equations 1, 2 and 3, respectively.

$$2Fe(NO_3)_3.9H_2O + Co(NO_3)_2.6H_2O + 4.5C_2H_5NO_2 + 0.25O_2 \rightarrow CoFe_2O_4 + 9CO_2 + 35.25H_2O + 6.25N_2 \quad (1)$$

$$2Fe(NO_3)_3.9H_2O + Co(NO_3)_2.6H_2O + 5.5C_2H_5NO_2 + 4.75O_2 \rightarrow CoFe_2O_4 + 11CO_2 + 37.75H_2O + 6.75N_2 \quad (2)$$

$$2Fe(NO_3)_3.9H_2O + Co(NO_3)_2.6H_2O + 3.5C_2H_5NO_2 \rightarrow CoFe_2O_4 + 7CO_2 + 32.75H_2O + 5.75N_2 + 4.25O_2 \quad (3)$$

The nitrates were individually dissolved in water and then mixed. The solution was stirred and heated for approximately 5 min. When reaching 60°C, the fuel that had previously been dissolved in water was added to the solution. The solution was maintained under stirring and temperature for a few minutes to promote perfect homogenization. The solution was placed in an electric muffle furnace preheated to 400°C until complete combustion (around 15 min).

2.2 *Chemical and structural characterization*

The crystallinity of the samples was evaluated by X-ray diffraction (XRD) using a PHILIPS diffractometer (model X'Pert MPD) at 40 kV and 40 mA using a Cu anode. The powder crystallite sizes were calculated using Scherrer's equation 4:

$$D = \frac{K\lambda}{\beta\ cos\theta} \quad (4)$$

where D represents the crystallite size, K is a constant that depends on the particle shape (we assume the particles to be spherical, meaning K=0.94), λ is the wavelength of the electromagnetic radiation used (1.5406 Å, a value related to the main characteristic radiation emitted by copper), θ is Bragg`s angle, and β is the contribution of the crystallite size to the full width at half maximum (FWHM) of the corresponding diffraction peak in radians.

The morphology of the $CoFe_2O_4$ was characterized by scanning electron microscopy (SEM) using a JEOL microscope (JSM 6060) with a maximum operating voltage of 30 kV and a nominal resolution of 3.5 nm. The applied voltage was 10 to 20 k.

3. Results and Discussions

The diffractograms in Figure1 shows the characteristic crystal peaks corresponding to the cobalt ferrite phase for all samples according to JCPDS 73-1960. The sample lean presented a high degree of purity and showed only the $COFe_2O_4$ phase. The stoichiometric and rich samples showed the formation of a second phase of cobalt oxide (JCPDS 73-1701).

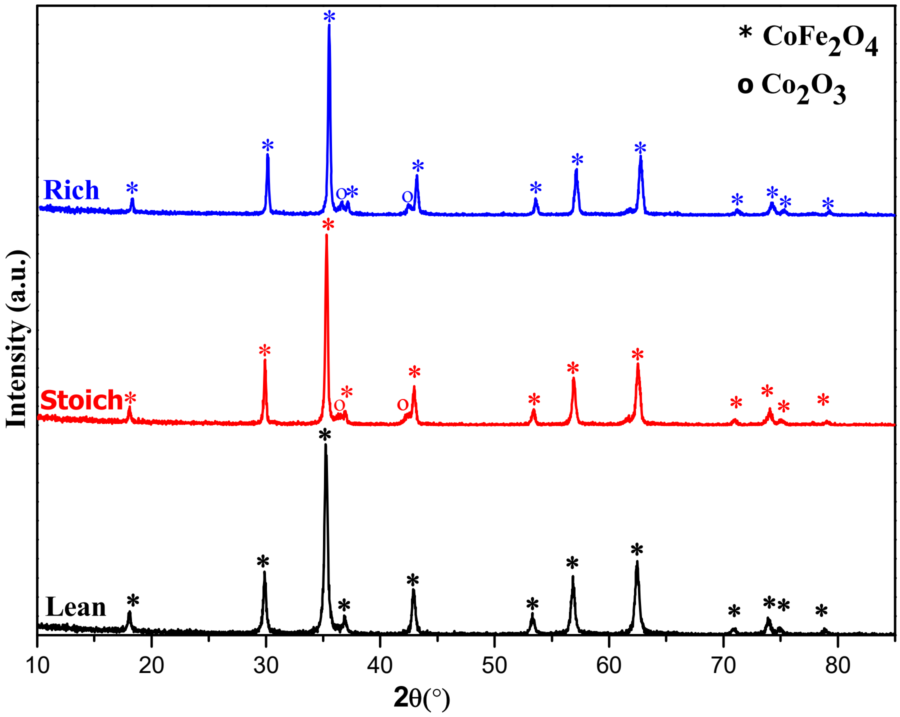

Figure 1. Diffractograms of the $CoFe_2O_4$ catalysts for different fuel concentrations.

SCS synthesis with elevated concentration of fuel leads to fast ignition and intense burn during reaction. With the excess of fuel, oxygen from the atmosphere is required in order to complete the reaction. This oxygen excess may cause the formation of secondary oxide phases besides the primary cobalt ferrite phase [21]. The crystallite sizes calculated by Scherrer`s for showed for the different concentrations: 23.58 nm for lean (the smallest size among all samples), 31.14 nm for stoichiometric, and 33.16 nm for Rich. These results indicate that powder has a nanostructured crystallite. Figure 2 shows SEM micrographs of the $CoFe_2O_4$ samples just after combustion with no grinding process involved.

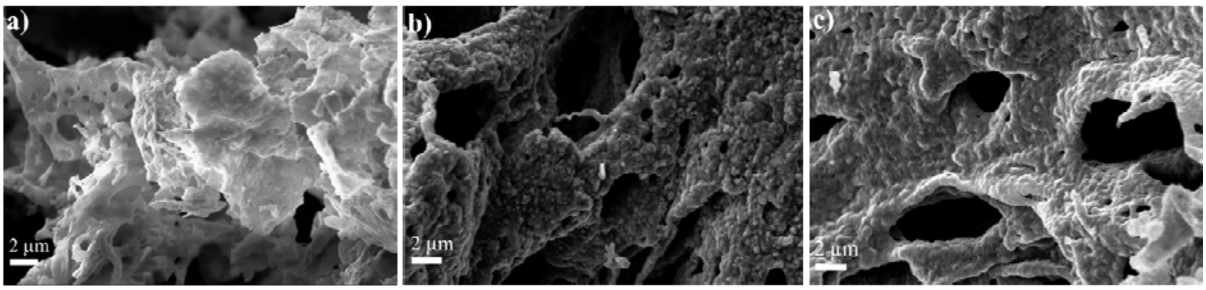

Figure 2. SEM images of samples: a) Lean, b) Stoich, c) Rich.

Figure 2 it is possible to observe the production of porous structures for all the compositions. The formation of the spongy features is attributed to the evolution of a large amount of gas during combustion [22].

The amount of oxygen involved in the reaction directly affects the velocity of the process and the product composition as discussed above. Glycine has a small carbonic chain, and the presence of N and OH in the structure provides an intense and fast high-temperature combustion during ignition, which releases a high volume of gases [21]. This release of gases leads to the production of more porous structures as can be seen when comparing the fuel-lean sample (Figure 2a) with the rich (Figure 2c) and stoichiometric sample (Figure 2b). It is possible to observe the increasing of structural porosity with the increasing of fuel concentration.

4. Conclusion

The synthetic route presented in this paper shown to be effective for production of nanostructured $CoFe_2O_4$. In this study was possible to conclude that in the SCS of $CoFe_2O_4$, higher concentrations of glycine lead to the formation of secondary phases of cobalt oxide. The fuel-lean sample was the only one that produced a nanometer pure phase of $CoFe_2O_4$. This sample is promising for applications in the electronics field, such as on solar-powered electric vehicles, since pure particles and good crystallinity are crucial in this area.

Acknowledgment

The authors would like to thank the Coordination for the Improvement of Higher Education Personnel - CAPES for the financial support. The present paper was presented inside the '*Toward a Sustainable Mobility*' special session as part of the '*Two Seats for a Solar Car*' research project, an action funded by the Italian Ministry of Foreign Affairs and International Cooperation within the Executive Programme of Cooperation in the field of Science and Technology between the Italian Republic and the Republic of Serbia.

References

[1] Carter, C. Barry, Norton M G 2007 *Ceramic Materials-Science and Engineering* (pringer Science & Business)

[2] Houshiar M, Zebhi F, Razi Z J, Alidoust A and Askari Z 2014 Synthesis of cobalt ferrite (CoFe2O4) nanoparticles using combustion, coprecipitation, and precipitation methods: A comparison study of size, structural, and magnetic properties, *J. Magn. Magn. Mater.* **371** 43–8

[3] Park B J, Choi K-H, Nam K C, Ali A, Min J E, Son H, Uhm H S, Kim H-J, Jung J-S and Choi E H 2015 Photodynamic Anticancer Activities of Multifunctional Cobalt Ferrite Nanoparticles in Various Cancer Cells, *J. Biomed. Nanotechnol.* **11** 226–35

[4] Yardımcı F S, Şenel M and Baykal A 2012 Amperometric hydrogen peroxide biosensor based on cobalt ferrite–chitosan nanocomposite, *Mater. Sci. Eng. C* **32** 269–75

[5] Rao G S N, Kumar S A, Rao K, Rao B P, Gupta A, Caltun O, Dumitru I and Kim C 2007 *Doped Cobalt Ferrites for Stress Sensor Applications*, 2007 2nd IEEE International Conference on Nano/Micro Engineered and Molecular Systems (IEEE), pp 1186–9

[6] Craciunescu C M, Kishi Y, De Graef M, Lograsso T A and Wuttig M R 2002 Cobalt-base ferromagnetic shape memory alloys ed C S Lynch pp 235–44

[7] Li X, Liu X, Lin C, Zhang H, Zhou Z, Fan G and Ma J 2019 Cobalt ferrite nanoparticles supported on drinking water treatment residuals: An efficient magnetic heterogeneous catalyst to activate peroxymonosulfate for the degradation of atrazine, *Chem. Eng. J.* **367** 208–18

[8] Caltun O, Dumitru I, Feder M, Lupu N and Chiriac H 2008 Substituted cobalt ferrites for sensors applications, *J. Magn. Magn. Mater.* **320** e869–73

[9] Hashemi M, Mohandes F, Salavati-Niasari M and Esmaeily A S 2015 Preparation of cobalt ferrite micro/nanoparticles by solid-state thermal decomposition of a novel single-source precursor, *J. Mater. Sci. Mater. Electron.* **26** 6860–7

[10] Qiu B, Deng Y, Du M, Xing M and Zhang J 2016 Ultradispersed Cobalt Ferrite Nanoparticles Assembled in Graphene Aerogel for Continuous Photo-Fenton Reaction and Enhanced Lithium Storage Performance, *Sci. Rep.* **6** 29099

[11] Minak G, Fragassa C and de Camargo F V 2017 *A brief review on determinant aspects in energy efficient solar car design and manufacturing*, International Conference on Sustainable Design and Manufacturing, Bologna, Italy, April 26 – 28, pp. 847-856

[12] de Camargo F V, Giacometti M and Pavlovic A 2017 *Increasing the energy efficiency in solar vehicles by using composite materials in the front suspension*, International Conference on Sustainable Design and Manufacturing, Bologna, Italy, April 26 – 28, pp. 801-811

[13] Minak G, Brugo T M, Fragassa C, Pavlovic A, de Camargo F V and Zavatta N 2019 Structural Design and Manufacturing of a Cruiser Class Solar Vehicle, *Journal of Visual Experiments* **143** e58525, doi:10.3791/58525

[14] Da Dalt S, Takimi A S, Volkmer T M, Sousa V C and Bergmann C P 2011 Magnetic and Mössbauer behavior of the nanostructured MgFe2O4 spinel obtained at low temperature, *Powder Technol.* **210** 103–8

[15] Zampiva R Y S, Kaufmann Junior C G, Pinto J S, Panta P C, Alves A K and Bergmann C P 2017 3D CNT macrostructure synthesis catalyzed by MgFe2O4nanoparticles—A study of surface area and spinel inversion influence, *Appl. Surf. Sci.* **422** 321–30

[16] Dinka P and Mukasayan A 2005 In situ preparation of Oxide-based Supported Catalysts by Solution Combustion Synthesis, *J. Phys. Chem. B* **109** 21627–33

[17] Giorgini L, Fragassa C, Zattini G and Pavlovic A 2016 Acid aging effects on surfaces of PTFE gaskets investigated by Fourier Transform Infrared Spectroscopy, *Tribology in Industry* **38**(3) 286-296.

[18] Fragassa C, Giorgini L, Pavlovic A and Zattini G 2016 Acid aging effects on surfaces of PTFE gaskets investigated by Thermal Analysis, *Tribology in Industry* **38(**4) 435-444

[19] Zattini G, Pavlovic A, Fragassa C and Giorgini L 2017 Characterization of solid residues emerging during ultrasonic cleaning treatments of tyre moulds, *FME Transactions* **45**(3) 339-347,

[20] Jain S R, Adiga K C and Pai Verneker V R 1981 A new approach to thermochemical calculations of condensed fuel-oxidizer mixtures, *Combust. Flame* **40** 71–9

[21] Jovanović R, Rašuo B, Stefanović P, Cvetinović D and Swiatkowski B 2013 Numerical investigation of pulverized coal jet flame characteristics under different oxy-fuel conditions, *Int. J. Heat Mass Transf.* **58** 654–62

[22] Effenberg G and Ilyenko S 2008 *Ternary Alloy Systems Phase Diagrams, Crystallographic and Thermo– dynamic Data* (German: Springer Berlin Heidelberg)